coatings

MDPI

Article

Investigation of the Structure and Properties of Molybdenum Coatings Produced by Laser-Directed Energy Deposition

Tatiana Tarasova [1,*], Marina Volosova [1], Andrey Skorobogatov [1], Sergey Voldemarovich Fedorov [1], Pavel Podrabinnik [1], Andrey Kholopov [2] and Sergey N. Grigoriev [1]

[1] Department of High-Efficiency Machining Technologies, Moscow State University of Technology "STANKIN", Vadkovsky Lane 3a, 127055 Moscow, Russia
[2] Laser Technologies in Manufacturing Department, The Bauman Moscow State Technical University, 2nd Bauman str. 5-1, 105005 Moscow, Russia
* Correspondence: tarasova952@mail.ru

Abstract: The paper considers the possibility of replacing the process of conventional vacuum brazing of a molybdenum plate on carbon steel using copper brazing with the process of laser-directed energy deposition of domestically produced molybdenum powder. The research task is motivated by the demand for removing low-melting copper brazing from molybdenum coatings on carbon steel. The parameters for the process of manufacturing molybdenum coatings using the additive technology of laser-directed energy deposition (LDED), which provides the required operational properties without further processing, have been developed. A study of the microstructure of the coating was carried out, including an examination of the distribution of the main elements over the depth of the coating. We established the preferred parameters of laser-directed energy deposition, which provide a high-quality deposited layer of Mo on the 25L carbon steel. The wear resistance of the coatings was examined following the «ball-on-disc» scheme according to the ASTM G99 standard. The results show that wear rate of the brazed Mo plate is higher than that of the deposited Mo layer on the 25L carbon steel substrate.

Keywords: laser-directed energy deposition; additive manufacturing; wear resistance; molybdenum powder; powder characterization; tribological properties; microstructure

check for updates

Citation: Tarasova, T.; Volosova, M.; Skorobogatov, A.; Fedorov, S.V.; Podrabinnik, P.; Kholopov, A.; Grigoriev, S.N. Investigation of the Structure and Properties of Molybdenum Coatings Produced by Laser-Directed Energy Deposition. *Coatings* **2023**, *13*, 1365. https://doi.org/10.3390/coatings13081365

Academic Editor: Robert B. Heimann

Received: 8 June 2023
Revised: 31 July 2023
Accepted: 1 August 2023
Published: 3 August 2023

Copyright: © 2023 by the authors. Licensee MDPI, Basel, Switzerland. This article is an open access article distributed under the terms and conditions of the Creative Commons Attribution (CC BY) license (https://creativecommons.org/licenses/by/4.0/).

1. Introduction

The prospects for the development of a machine-building complex are largely associated with the development of additive manufacturing (AM), which combines technologies for manufacturing free-shaped parts based on three-dimensional CAD models without the use of forming operations and machining. Additive technologies (AT) are considered to be alternatives to conventional processing techniques. The main features of AT are given in terms and definitional standards developed by ASTM [1]. These technologies include, for instance, powder bed fusion–laser beam (PBF-LB) and laser-directed energy deposition (LDED) [1,2]. Additionally, the list of materials applied in AM continues to grow rapidly. In addition to methods of producing metal alloys, technologies for the manufacture of ceramic products are being developed [3,4].

Over the last years, three-dimensional shaping by the LDED technology has been undergoing intensive development. This method of processing uses laser radiation energy to melt the added material and the underlying layer in order to form a deposited bead on it that is metallurgically bonded to the substrate. The relative movement of the laser beam and the substrate allows the depositing of the material in a plane along the intended trajectory. Repeating the step layer-by-layer along the z axis makes it possible to obtain 3D free-shaped objects. LDED, performed at optimal parameters, ensures strong adhesion in the boundary zone and coatings with the required properties.

Recently, researchers have expressed great interest in the creation of deposited coatings from molybdenum (Mo) and its alloys since there is great demand for improving the performance of the bimetallic parts and coatings produced from molybdenum-based alloys. This interest is driven by the unique complex of properties of Mo: high melting temperature, high strength at elevated temperatures, low thermal expansion, and high thermal and electrical conductivity. In this regard, studies of the creation of bimetallic products and coatings from powders of molybdenum and its alloys, performed using additive technologies such as PBF-LB and LDED, are especially relevant. Vasiltsov et al. used pure (>99%) fine Mo powder to obtain molybdenum coatings via LDED and adopted the following working parameters: scanning speed V = 0.8 cm/s, cladding distance d = 0.3 cm, and laser power P = 2 kW [5]. It was calculated that 51% of power is consumed for powder evaporation. Within the study, a homogeneous Mo structure was achieved to facilitate good performance properties.

Research in this area shows that there are a number of problems in obtaining products with high density and a lack of cracks from molybdenum using these methods [6,7]. It is reported that cracking can be reduced by introducing several elements. Thus, Fichtner et al. developed the LDED parameters for achieving a Mo-Si-B alloy without cracks [8]. Guo et al. investigated the Mo-Si-B alloy obtained via PBF-LB technology and measured the density and mechanical properties at various process parameters and different ratios of the alloy components [9]. The highest density of 94.22% was achieved for Mo93.5-Si4.5-B2.0 alloy at a laser power of 250 W, laser scanning velocity of 500 mm/s, and powder layer thickness of 60 μm. Pure Mo powder has also been utilized with PBF-LB technology. Yan et al. concluded that a high melting point and transition temperature stand behind the obstacles in the formation of fine defect-free microstructures via selective laser melting [10]. The authors were able to achieve stable beads of Mo with low porosity and cracking within the linear energy density interval from 0.44 kJ/mm to 0.64 kJ/mm. The highest density of pure Mo specimens obtained was reported to be 99.1%.

Alloying is considered to be a promising method for obtaining defectless refractory metal parts using PBF-LB. In the study [11], the authors used pure Mo powder and Mo powder alloyed with carbon for PBF-LB. It was shown that doping molybdenum with carbon in the amount of 0.45 wt. % makes it possible to produce parts from molybdenum using PBF-LB without cracks and with mechanical properties comparable to those of molybdenum products obtained conventionally. To avoid cracking and achieve a density up to 99.7% (theoretical density is 10.08 g/cm^3), the authors suggest heating the substrate during the PBF-LB process up to 800 °C. The authors claim that when alloyed with 0.45 wt. % carbon, molybdenum achieves an average 3-point bending strength 340% higher than that of pure molybdenum produced using PBF-LB.

Much more research on the PBF-LB is focused on tungsten than the small number of studies that center on molybdenum. However, the defects found in the AM products derived from tungsten and molybdenum are very similar [12–18]. A significant proportion of defects such as micropores or microcracks arises primarily due to the non-optimized parameters of the AM processes. Roh et al. developed LDED parameters for the deposition of Mo coatings with low porosity (<2%) [18]. However, an attempt to fully eliminate porosity failed as cracking expanded instead. In [19], Johnson et al. showed the possibility of Mo part production using laser- and electron beam-directed energy deposition. Nevertheless, it is admitted that the ways of improving microstructure to reduce porosity and cracking need further study.

To improve static and dynamic mechanical properties, hot isostatic pressing (HIP) is being used as a post-treatment method. Previous studies show that defects in products made from various metal powders using PBF-LB are significantly reduced with HIP [20,21]. The method is promising for improving the quality of parts made of Mo alloys obtained by AM, given that AM process parameters are optimal. On the other hand, production costs increase drastically when using this method.

Overall, according to the review, research in the field of processing molybdenum using AT is promising. However, the data on the properties of molybdenum coatings obtained using LDED are insufficient for further implementation in the industry. Considering the trend of replacing the low-melting copper brazing needed to manufacture refractory Mo coatings, it is necessary to continue the research in that field.

The current research aims to develop the parameters of the process of manufacturing molybdenum coatings using LDED, which provides the required properties without further processing.

2. Materials and Methods

2.1. Raw Materials

Previously, the possibility of replacing copper brazing via the deposition of Mo powder onto a steel substrate was shown in [22,23]. This made it possible to exclude the low-melting interlayer from the coating structure, to avoid its destruction, and thus to provide high wear resistance at elevated temperatures. This research extends the obtained results and focuses on the development of process parameters for the manufacture of molybdenum coatings on carbon steel using LDED to provide the required wear resistance.

A mass of 25L of carbon steel was chosen as a substrate material (Table 1). Molybdenum powder PMS-M99.9 (JSC "Polema", Tula, Russia) was taken as a raw material for use in the LDED process. The Mo powder was manufactured by mechanical disintegration, followed by plasma spheroidization. Particle size distribution ranged from 40 μm to 100 μm with a spherical shape. The chemical composition and properties of the powder are given in Tables 2 and 3, respectively [22].

Table 1. The chemical composition of the 25L steel substrate.

Material	Elements Composition, % Mass					
	Fe	C	Mn	Si	S	P
25L steel	Balance	0.30	0.54	0.51	0.019	0.024

Table 2. The chemical composition of the Mo powders PMS-M99.9 and PM-M.

Material	Elements Composition, % Mass		
	Mo	Metal Impurities [1], Total	O
PMS-M99.9	Balance	0.1	0.025

[1] Al, Fe, K, Ca, Si, W, Mg, Ni, Na, Mn, and Zn.

Table 3. The properties of Mo powders PMS-M99.9 and PM-M.

Material	Flowability, s	Packed Density, g/cm^3	Tap Density, g/cm^3
PMS-M99.9	10.4	6.4	7.14

In order to confirm the compliance of the raw powders with the required parameters specified in the standards for additive technologies, as well as to verify the parameters declared by the manufacturer, an input control of the powder materials was carried out. Granulometric analysis of powders was carried out on an Occhio 500 Nano optical morphometer (Occhio S.A., Liege, Belgium) with software for statistical image analysis (Figure 1). Morphological and elemental analyses were performed on a Tescan Vega 3 LMH scanning electron microscope (SEM) (Tescan, Brno, Czech Republic) equipped with an energy-dispersive X-ray microanalyzer (Oxford Instruments, Abington, UK). Based on the results of the granulometric analysis of powder grade PMS-M99.9, integral and differential curves of the distribution of powder particles were constructed by size (Figure 1).

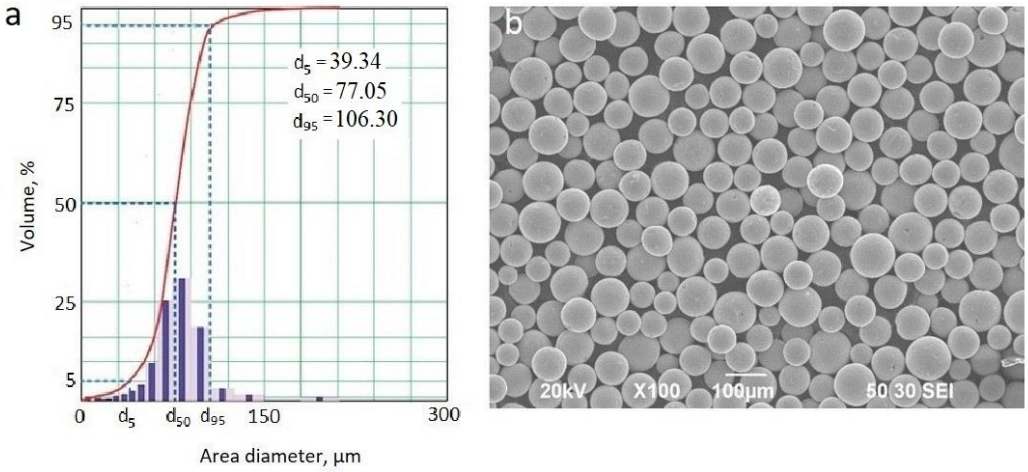


Figure 1. (**a**) Integral curve and particle size distribution histogram of PMS-M99.9 powder; (**b**) surface morphology of powder particles [18].

The size distribution of powder particles is described by the Gaussian normal distribution law. It was found that the average particle size of the PMS-M99.9 powder was d_{med} = 76.79 µm, and that the volume of particles that did not correspond to the size of the main fraction declared by the manufacturer (from 40 to 100 µm) was 9.75% [22]. The sphericity shape factor was >90%. Thus, the PMS-M99.9 Mo powder meets the requirements for the LDED process [22].

2.2. LDED Equipment

LDED process was carried out on an installation equipped with a multimode ytterbium fiber laser IPG (IPG Photonics, Fryazino, Russia) with a power of 3000 W [22]. Technical data are given in Table 4.

Table 4. LDED equipment technical data.

№	Parameter	Value
1	Building zone size, mm	400 × 400 × 400
2	Number of axes	5
3	Positioning accuracy, mm/m	0.03
4	Laser wavelength, µm	1.07
5	Laser wavelength, µm	<3000
6	Lens focus distance, mm	200
7	Min. laser spot diameter, µm	1200
8	Feedstock powder particle size, µm	40–200
9	Powder consumption, g/min	<300

2.3. Material Characterization Methods

The microstructure and surface relief of the specimens were studied using a Carl Zeiss Axio Observer D1m optical microscope (Carl Zeiss Microscopy GmbH, Jena, Germany) and a PHENOM G2 PRO scanning electron microscope (ThermoFisher Scientific, Pfeddersheim, Germany) with an integrated energy-dispersive analysis (EDX) module.

The phase composition of the samples was determined using the PANalytical Empyrean X-ray diffractometer (Malvern Panalytical Inc., Westborough, MA, USA) with CuKa radiation. The obtained XRD patterns were processed through the PANalytical High Score Plus software (v3.0e) [24] and ICCD PDF-2 and COD databases [25] to reveal the phase composition.

The microhardness was tested by the Qness Q10A tester (Qness GmbH, Golling, Austria) with a maximum indentation load of 10 kg, providing a Vickers method analysis measurement error of 0.01 HV.

Sample density was determined by hydrostatic weighing on a Mettler Toledo XP504 (Mettler Toledo AG, Greifensee, Switzerland) balance with an accuracy of 0.001 g/cm^3. Ethyl alcohol was used as the working fluid.

The wear resistance of the material was tested on the Microtest MT/60/NI tribometer (Microtest, Madrid, Spain) according to the ball-on-disc scheme following the ASTM G99 standard (Figure 2). For the experiment, flat 19 × 19 × 8 mm plates were prepared for sliding against the 6 mm Al_2O_3 ball. At the preferential LDED parameters, there were 3 specimens made for the tests. The test conditions were as follows: load F = 10 N, rotating speed W = 200 rpm, and sliding distance S = 94 m. During the test, sliding friction force is continuously recorded, and the value of the coefficient of friction is automatically calculated to display the live graphs. To estimate the wear, the linear dimensions of the friction pair are measured before and after the test. The task is addressed by analyzing track profiles using a three-dimensional surface profilometer, namely, Taylor Hobson's Talysurf. It restores the surface morphology by mechanically bringing the needle into contact with the sample at a step of 0.01 μm and a scanning step at a speed of 0.1 mm/s. Once the topography assessing is finished, volume loss is derived, and wear rate is calculated according to the Equation (1):

$$W = V/(F \times S), \quad (1)$$

where V is the volume loss after the tests (mm^3), F is the applied load (N), and S is the sliding distance (m).

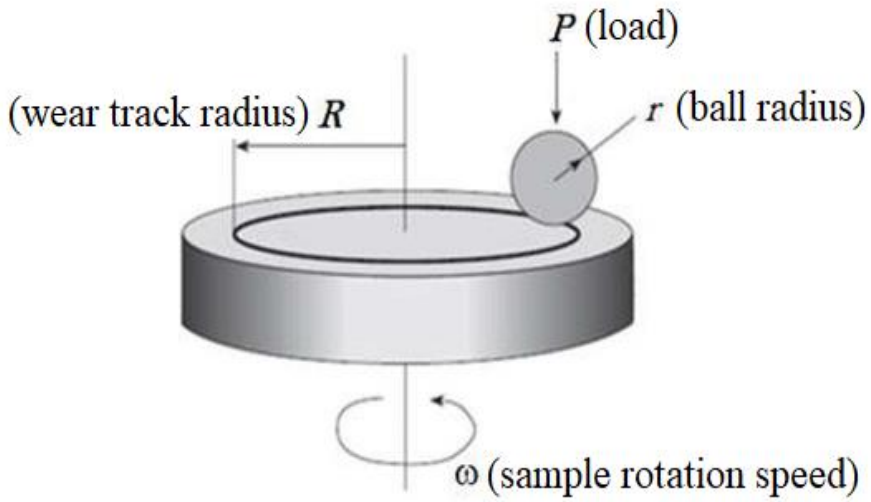


Figure 2. The ball-on-disc tribological testing scheme.

3. Results and Discussion

3.1. The Investigation of Microstructure of the Molybdenum Coatings on the 25L Carbon Steel

Previous studies found the preferential parameters for performing LDED of Mo powder on the 25L cast steel based on the microstructural analysis of cross sections of single beads and their geometrical appearance. These parameters were height, width, penetration depth and hardness. The technological parameters included laser power P = 480 W, scanning speed V = 400 mm/min, powder consumption rate F_{pow} = 4 g/min, carrier gas flow F_{gas} = 4 L/min, and shield gas flow F_{shgas} = 10 L/min [22]. This work continues the investigation of Mo coatings of different thicknesses on the 25L steel with vertical step $\Delta z \approx 0.25$ mm. To improve the quality of the coating, laser radiation power was varied during the LDED process. For the first layer, the laser irradiation power was set to P = 500 W, for the second layer P = 900 W, and for the following layers P = 1000 W (Table 5).

Table 5. LDED technological parameters of Mo deposition on the 25L steel.

Sample	Laser Irradiation Power, W	Scanning Speed, mm/min	Powder Consumption, g/min
a	1st layer—500 2nd layer—900 3rd and the following layers—1000	300	6
b		300	4
c		400	6
d		400	4
e	500	400	4

The study of the microstructure and porosity of the obtained coatings showed that with an increase in the laser radiation power during the LDED process according to the abovementioned laser power values, a scanning speed of 400 mm/min and a powder consumption of 4 g/min, high-quality coatings are obtained with no cracks and low porosity, as expressed by a pore size of less than 100 µm (Figures 3d and 4d).

Optical and electron microscopy of the LDED layers showed that it is possible to achieve a high-quality layer without pores and cracks (Figures 5–7). This is explained not only by the selection of preferred processing parameters, but also by the presence of carbon in the deposited layer (Figure 6), which dissolves in the melt pool during the cladding of molybdenum powder onto carbon steel in accordance with the Marangoni effect. XRD analysis showed the presence of molybdenum carbide Mo_2C in the deposited layer, which contributes to grain refinement during the solidification of Mo. Furthermore, compared to the use of pure Mo, a Mo-C system solidifies at an interval of temperatures, not at a constant temperature. This gives time for the melt to fill all the voids during cooling. Thus, it contributes to forming crack-free microstructure during solidification, which is consistent with the conclusions in [22].

The hardness and density of the obtained samples are presented in Table 6. It also contains data on the conventionally obtained Mo coatings on the 25L steel (vacuum brazing with copper) in order to compare the results.

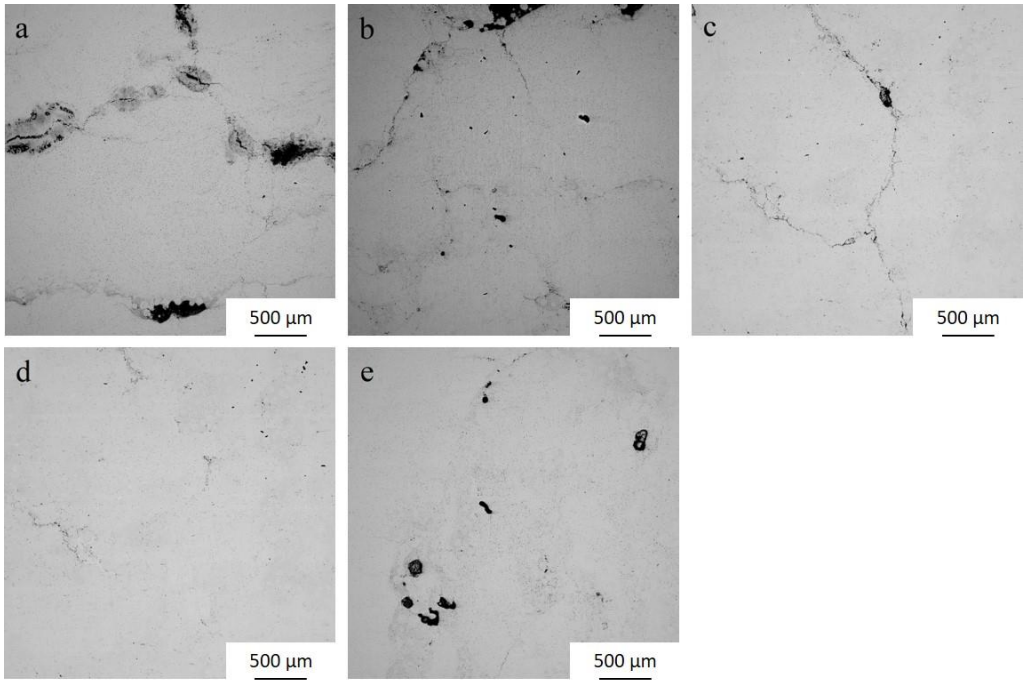


Figure 3. SEM images the microstructure of the deposited Mo layers on the 25L steel (×100). Images (**a**–**e**) correspond to the samples and working parameters in Table 5. Image (**d**) shows low-porosity microstructure with pore size <100 µm.

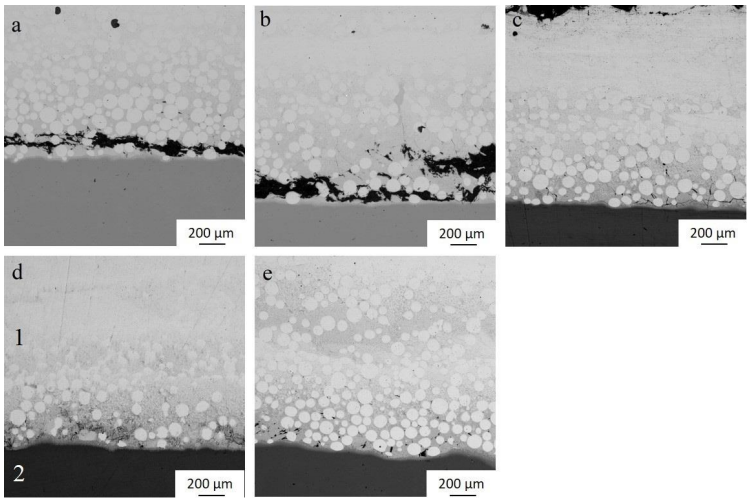


Figure 4. SEM images of the cross section microstructure of the deposited Mo coatings on the 25L steel (×200). Images (**a**–**e**) correspond to the samples and working parameters in Table 5. Designations: 1–4 mm thick deposited LDED coating; 2–10 mm thick 25L steel substrate.

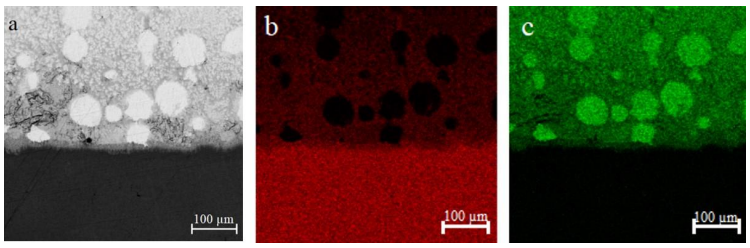


Figure 5. The microstructure of the LDED Mo layer onto the 25L steel near the boundary of the melt pool: (**a**) Electron image; (**b**) Fe distribution map; (**c**) Mo distribution map.

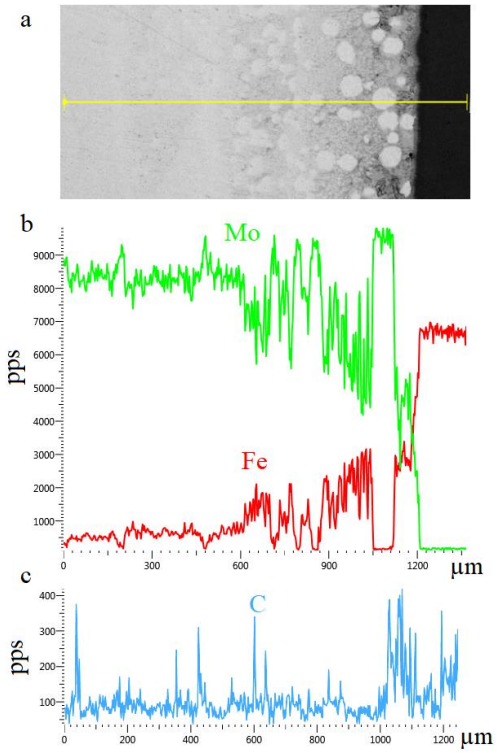


Figure 6. The content of the main components in the deposited layer along the line: (**a**) Electron image; (**b**) Fe and Mo distribution; (**c**) Carbon distribution.

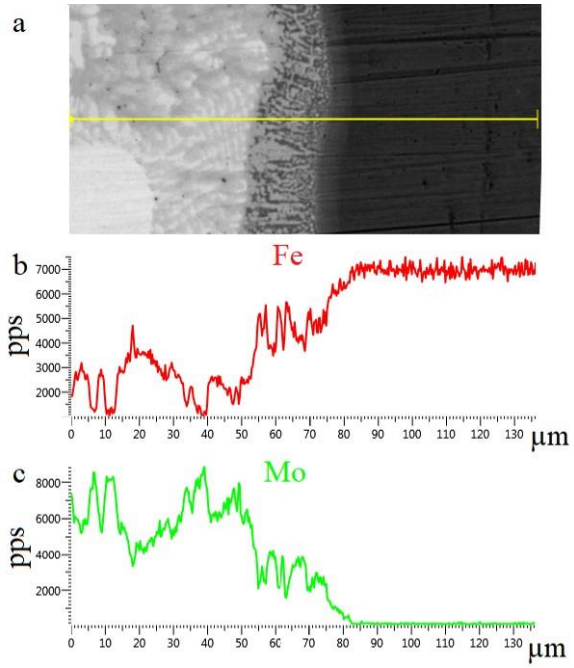


Figure 7. The content of the main components in the transition layer of the LDED Mo layer onto steel 25L: (**a**) Electron image; (**b**) Fe distribution; (**c**) Mo distribution.

Table 6. The results of hardness testing, density measurements and wear rate of Mo plate and deposited Mo layer obtained using LDED.

Technology	Hardness, HV	Density, g/cm^3	Wear Rate W, mm^3/Nm
Vacuum brazing (t = 1120 °C, τ = 10 min)	182–192	10.0–10.2	4.9245×10^{-4}
LDED of the PMS-99.9M Mo powder (Table 5, mode d)	423–470	9.9–10.1	3.0529×10^{-4}

The study of the distribution of molybdenum and iron in the near-boundary areas of the deposited layer shows a steady reduction in the concentration of molybdenum in the transition to the substrate of the steel 25L, as well as the mutual diffusion of iron and carbon into the deposited molybdenum layer (Figures 5 and 6). These occurrences ensure the good adhesion of the LDED layer to the substrate.

The microstructure images show the distinctive spherical inclusions of molybdenum of different diameters, which crystallize primarily from the liquid phase, and uniaxial dendritic inclusions. In the transition layer directly adjacent to the substrate, the dendrites crystallize in the direction of heat removal (Figure 7a).

3.2. Tribologcal Tests of the Molybdenum LDED Coatings

The study of wear resistance was carried out on samples made using LDED of molybdenum on steel 25L according to the parameters (Table 5, sample d) and samples obtained by brazing Mo plates on steel 25L using copper solder. The Mo plates were obtained conventionally. Tribological tests were carried out for both LDED and brazing coatings in order to compare their behavior in operating conditions.

The analysis of the graphic dependencies of the friction coefficients shows that the coefficient of friction of the deposited layers is lower than that of the brazed molybdenum plate (Figure 8, ~0.47 and ~0.67, respectively). The run-in period is approximately the same for both samples.

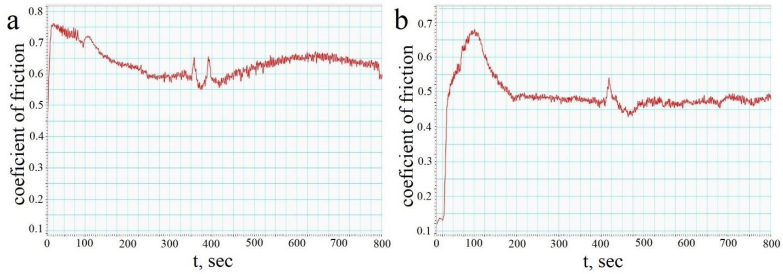


Figure 8. The dependence of the friction coefficient on the operating time: (**a**) brazed molybdenum plate; (**b**) LDED molybdenum layer.

From the graphs presented in Figure 9, it can be seen that for the deposited specimens wear after the running-in period is lower than that for the brazed molybdenum plate. The running-in period is also much shorter.

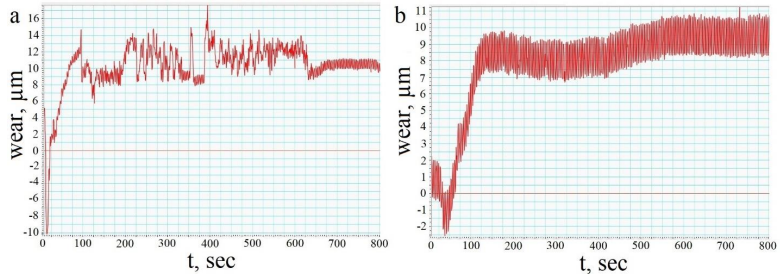


Figure 9. The dependence of wear on the operating time: (**a**) brazed molybdenum plate; (**b**) LDED molybdenum layer.

Figure 10 shows the surface topography of the 3D wear tracks for a brazed Mo plate and a deposited Mo powder after sliding tests against the Al_2O_3 ball. The wear rate (mm^3/Nm) of the Mo plate and the deposited Mo layer were estimated based on the 3D surface topography of the wear paths and the results are presented in Table 6. The results demonstrate that the wear of the brazed Mo plate is higher than that of the deposited Mo layer by about 1.3 times. This is due to the fact that the deposited layer developed a finer microstructure owing to the fast cooling rates during LDED and the appearance of a small amount of molybdenum carbide (Mo_2C).

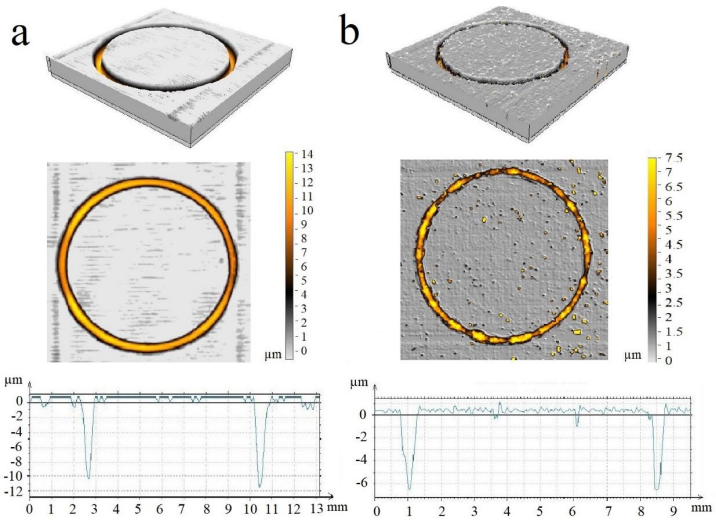


Figure 10. The three-dimensional topographies and a top view of wear paths: (**a**) Mo plate brazed to steel; (**b**) LDED deposited Mo layer on 25L steel. Technological parameters set d, according to the Table 5. Wear depth is shown on the color scale, V = 200 rpm, F = 10 N, S = 94 m.

4. Conclusions

Within the research, the microstructure of a coating obtained using LDED of the domestically produced Mo powder on 25L carbon steel was studied. The preferred technological regimes for the LDED process were found to ensure the production of high-quality coatings without defects such as cracks and pores.

Studies of the distribution of molybdenum and iron in the near-boundary areas of the deposited layer show a gradual decrease in the concentration of Mo upon transition to the substrate of steel 25L and the mutual diffusion of iron and carbon into the deposited molybdenum layer. These effects ensure the strong bonding of the LDED material to the substrate.

Furthermore, we carried out tribological tests to the assess wear resistance of the LDED and vacuum-brazed Mo coatings. It was established that the wear resistance of the Mo layer deposited on the 25L carbon steel was higher than that obtained by vacuum brazing.

Thus, the prospects of replacing the conventional process of vacuum brazing of Mo plates on steel with low-melting copper soldering via the LDED of Mo powder have been shown.

Author Contributions: Conceptualization, T.T.; methodology, T.T. and A.S.; software, A.S.; validation, A.S., P.P. and T.T.; formal analysis, M.V. and S.V.F.; investigation, A.S. and A.K.; resources, A.S., A.K. and S.V.F.; data curation, M.V.; writing—original draft preparation, T.T.; writing—review and editing, T.T. and P.P.; visualization, A.S. and P.P.; supervision, S.N.G.; project administration, M.V.; funding acquisition, M.V. All authors have read and agreed to the published version of the manuscript.

Funding: This work was funded by the state assignment of the Ministry of Science and Higher Education of the Russian Federation, Project No. FSFS-2023-0003.

Institutional Review Board Statement: Not applicable.

Informed Consent Statement: Not applicable.

Data Availability Statement: Data sharing not applicable.

Acknowledgments: The study was carried out on the equipment of the Center of Collective Use "State Engineering Center" of MSUT "STANKIN" supported by the Ministry of Higher Education of the Russian Federation (project 075-15-2021-695 from 26 July 2021, unique identifier RF 2296.61321X0013).

Conflicts of Interest: The authors declare no conflict of interest.

References

1. *ISO/ASTM 52900:2021*; Additive Manufacturing—General Principles—Fundamentals and Vocabulary. International Organization for Standarization: London, UK, 2021. Available online: https://www.iso.org/standard/74514.html?browse=tc (accessed on 16 February 2023).
2. Grigoriev, S.N.; Tarasova, T.V. Possibilities of the technology of additive production for making complex-shape parts and depositing functional coatings from metallic powders. *Met. Sci. Heat Treat.* **2016**, *57*, 579–584. [CrossRef]
3. Khmyrov, R.S.; Grigoriev, S.N.; Okunkova, A.A.; Gusarov, A.V. On the possibility of selective laser melting of quartz glass. *Phys. Procedia* **2014**, *56*, 345–356. [CrossRef]
4. Khmyrov, R.S.; Protasov, C.E.; Grigoriev, S.N.; Gusarov, A.V. Crack-free selective laser melting of silica glass: Single beads and monolayers on the substrate of the same material. *Int. J. Adv. Manuf. Technol.* **2016**, *85*, 1461–1469. [CrossRef]
5. Vasiltsov, V.V.; Galushkin, M.G.; Iliechev, I.N.; Misyurov, A.I.; Panchenko, V. Layer-wise metal-powder laser surfacing: Analytical theory and experiment. *Vestnik MGTU Im. N.E. Baumana* **2012**, *6*, 69–77.
6. Higashi, M.; Ozaki, T. Selective laser melting of pure molybdenum: Evolution of defect and crystallographic texture with process parameters. *Mater. Des.* **2020**, *191*, 108588. [CrossRef]
7. Alinejadian, N.; Wang, P.; Kollo, L.; Prashanth, K.G. Selective laser melting of commercially pure molybdenum by laser rescanning. *3D Print. Addit. Manuf.* **2022**. [CrossRef]
8. Fichtner, D.; Schmelzer, J.; Yang, W.; Heinze, C.; Krüger, M. Additive manufacturing of a near-eutectic Mo–Si–B alloy: Processing and resulting properties. *Intermetallics* **2020**, *128*, 107025. [CrossRef]
9. Guo, Z.; Han, R.; Li, Y.; Zhu, Y.; Zhang, B.; Zhang, H. Mo-Si-B Alloy Formed by Optional Laser Melting Process. *J. Environ. Anal. Chem.* **2022**, *2022*, 4996265. [CrossRef]

10. Yan, A.; Atif, A.M.; Wang, X.; Lan, T.; Wang, Z. The Microstructure and Cracking Behaviors of Pure Molybdenum Fabricated by Selective Laser Melting. *Materials* **2022**, *15*, 6230. [CrossRef]
11. Kaserer, L.; Braun, J.; Stajkovic, J.; Leitz, K.-H.; Tabernig, B.; Singer, P.; Letofsky-Papst, I.; Kestler, H.; Leichtfried, G. Fully dense and crack free molybdenum manufactured by Selective Laser Melting through alloying with carbon. *Int. J. Refract. Metals Hard Mater.* **2019**, *84*, 105000. [CrossRef]
12. Priyanshu, B. SLM Manufacturing of Molybdenum. Ph.D. Dissertation, The University of Sheffield, Sheffield, UK, 2016.
13. Zhou, W.; Sun, X.; Tsunoda, K.; Kikuchi, K.; Nomura, N.; Yoshimi, K.; Kawasaki, A. Powder fabrication and laser additive manufacturing of MoSiBTiC alloy. *Intermetallics* **2019**, *104*, 33–42. [CrossRef]
14. Zhou, X.; Liu, X.; Zhang, D.; Shen, Z.; Liu, W. Balling phenomena in selective laser melted tungsten. *J. Mater. Process. Technol.* **2015**, *222*, 33–42. [CrossRef]
15. Tan, C.; Zhou, K.; Ma, W.; Attard, B.; Zhang, P.; Kuang, T. Selective laser melting of high-performance pure tungsten: Parameter design, densification behavior and mechanical properties. *Sci. Technol. Adv. Mater.* **2018**, *19*, 370–380. [CrossRef]
16. Kurzynowski, T.; Smolina, I.; Kurzac, J.; Chlebus, E. Selective Laser Melting of Pure Tungsten. In Proceedings of the 3rd Fraunhofer Direct Digital Manufacturing Conference, Berlin, Germany, 16–17 March 2016.
17. Iveković, A.; Omidvari, N.; Vrancken, B.; Lietaert, K.; Thijs, L.; Vanmeensel, K.; Vleugels, J.; Kruth, J.P. Selective laser melting of tungsten and tungsten alloys. *Int. J. Refract. Met. Hard Mater.* **2018**, *72*, 27–32. [CrossRef]
18. Roh, G.W.; Park, E.S.; Moon, J.; Lee, H.; Byun, J. Direct energy Deposition of Mo powder prepared by electrode in Duction Melting gas atomization. *Arch. Metall. Mater.* **2021**, *66*, 795.
19. Johnson, J.L.; Palmer, T. Directed energy deposition of molybdenum. *Ijrmhm* **2019**, *84*, 105029. [CrossRef]
20. Tillmann, W.; Schaak, C.; Nellesen, J.; Schaper, M.; Aydinöz, M.U.; Hoyer, K.P. Hot isostatic pressing of IN718 components manufactured by selective laser melting. *Addit. Manuf.* **2017**, *13*, 93–102. [CrossRef]
21. Harrison, N.J.; Todd, I.; Mumtaz, K. Reduction of micro-cracking in nickel superalloys processed by Selective Laser Melting: A fundamental alloy design approach. *Acta Mater.* **2015**, *94*, 59–68. [CrossRef]
22. Metel, A.S.; Tarasova, T.; Skorobogatov, A.; Podrabinnik, P.; Volosova, M.; Grigoriev, S.N. Quality Diagnostics of Parts Produced by Combined Additive Manufacturing Technology. *Metals* **2023**, *13*, 19. [CrossRef]
23. Metel, A.S.; Tarasova, T.; Skorobogatov, A.; Podrabinnik, P.; Melnik, Y.; Grigoriev, S.N. Feasibility of Production of Multimaterial Metal Objects by Laser-Directed Energy Deposition. *Metals* **2022**, *12*, 1566. [CrossRef]
24. Shelekhov, E.V.; Sviridova, T.A. Programs for X-ray analysis of polycrystals. *Metal Sci. Heat Treat.* **2000**, *42*, 309–313. [CrossRef]
25. Gražulis, S.; Chateigner, D.; Downs, R.T.; Yokochi, A.F.T.; Quirós, M.; Lutterotti, L.; Manakova, E.; Butkus, J.; Moeck, P.; Le Bail, A. Crystallography Open Database–an open-access collection of crystal structures. *J. Appl. Cryst.* **2009**, *42*, 726–729. [CrossRef] [PubMed]

Disclaimer/Publisher's Note: The statements, opinions and data contained in all publications are solely those of the individual author(s) and contributor(s) and not of MDPI and/or the editor(s). MDPI and/or the editor(s) disclaim responsibility for any injury to people or property resulting from any ideas, methods, instructions or products referred to in the content.